Two Polymeric Linear Tri-nickel(II) Complexes: $[Ni_3(\mu_3\text{-dpa})_4(C_4O_4Me)]_n(BF_4)_n$ and $[Ni_3(\mu_3\text{-dpa})_4(N_3)]_n(PF_6)_n$ Synthesis, Structural Characterization and Magnetic Properties

Chi-How Peng[a] (彭之皓), Chih-Chieh Wang[a,b] (王志傑), Hsiao-Ching Lee[a] (李曉菁), Wei-Chung Lo[a] (駱韋仲), Gene-Hsiang Lee[a] (李錦祥) and Shie-Ming Peng[a]* (彭旭明)
[a]*Department of Chemistry, National Taiwan University, Taipei, Taiwan, R.O.C.*
[b]*Department of Chemistry, Soochow University, Taipei, Taiwan, R.O.C.*

Two new linear tri-nickel(II) complexes with an infinite polymeric chain, $[Ni_3(\mu_3\text{-dpa})_4(C_4O_4Me)](BF_4)$ **1** and $[Ni_3(\mu_3\text{-dpa})_4(N_3)](PF_6)$ **2**, [dpa$^-$ = di(α-pyridyl)amido anion], have been synthesized and their structures were determined by X-ray diffraction. Compound **1** crystallizes in the monoclinic system, space group *C* 2/c, with a = 19.9078(3), b = 13.2986(2), c = 37.6622(5) Å, β = 94.091(1)°, Z = 8. Compound **2** crystallizes in the monoclinic system, space group P 2_1/n, with a = 13.323(4), b = 23.217(3), c = 17.528(5) Å, β = 94.42(3)°, Z = 4. The two complexes are described as one-dimensional systems with the $(C_4O_4Me)^-$, **1**, or N_3^-, **2**, serving as a μ-(1,3) bridged ligand at the two axial sites of each $[Ni_3(\mu_3\text{-dpa})_4]^{2+}$ fragment. The Ni-Ni distances of 2.400(1) and 2.402(1) in **1** and 2.389(2), 2.385(2) in **2** are obviously shorter than those of 2.4325(7), 2.4356(7) in the monomeric complex $[Ni_3(\mu_3\text{-dpa})_4(N_3)_2]$ **3**. The magnetic properties of complexes **2** and **3** were studied by susceptibility measurements *vs* temperature. The χ_M *vs* T plots of both complexes show a strong anti-ferromagnetic behavior. The simulated J_{13} values are -95 cm^{-1} and -97 cm^{-1} for **2** and **3**, respectively.

INTRODUCTION

Since 1991 when the structural description of the first linear trinickel complex, $[Ni_3(\mu_3\text{-dpa})_4Cl_2]$, was reported,[1a] a number of trinuclear metal string complexes with various metal centers, $[M_3(\mu_3\text{-dpa})_4Cl_2]$; M = Ru,[2] Rh,[2] Cr,[3] Co,[4] Ni,[1] and Cu,[5] have been synthesized and studied. Their syntheses, structures, spectra and magnetic properties have provided much information on the understanding of the M-M bonding beyond dinuclear complexes.[1-5] Furthermore, the number of metal ions in a linear oligo-nuclear metal string complex has been successfully lengthened from three,[1-5] four,[6] five,[7,8] seven,[6,9] to nine metal ions.[10] The potential as a molecular metal wire for oligo-nuclear linear metal string complexes has become an important and interesting topic. In the previous reports, the axial ligand Cl$^-$ in the $[M_3(\mu_3\text{-dpa})_4Cl_2]$ and $[M_5(\mu_5\text{-tpda})_4Cl_2]$ complexes (M = Cr, Co, Ni) can be easily replaced by other ligands.[7,8] Therefore, the $[M_3(\mu_3\text{-dpa})_4]^{2+}$ or $[M_5(\mu_5\text{-tpda})_4]^{2+}$ ions can be considered as a building block with two vacant coordination sites. If some polydentate ligands are added, they can be self-assembled to form one-, two-, or even three-dimensional polymeric compounds as shown in Scheme I. In this study, two polymeric complexes,

Scheme I

One Dimensional Polymeric Metalwire

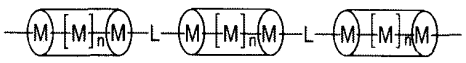

Two Dimensional Polymeric Network Metalwire

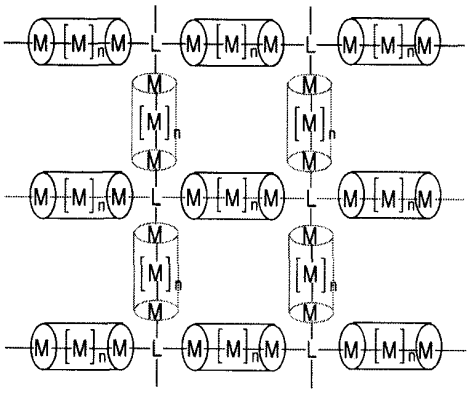

$[Ni_3(\mu_3\text{-dpa})_4(\mu_{1,3}\text{-}C_4O_4(Me))](BF_4)$ **1**, $[Ni_3(\mu_3\text{-dpa})_4(\mu_{1,3}\text{-}N_3)](PF_6)$ **2**, and one monomer, $[Ni_3(\mu_3\text{-dpa})_4(\mu_1\text{-}N_3)_2]$ **3** were

Dedicated to Professor Sheng-lieh Liu on the occasion of his ninetieth birthday.

* Corresponding author. Tel: +886-2-23630231 ext. 2111; Fax: +886-2-23636359; E-mail: smpeng@mail.ch.ntu.edu.tw

successfully synthesized. Their structures are described and discussed in detail. Meanwhile, the magnetic susceptibility measurements of two azide-bonded complexes, **2** and **3**, are also reported.

EXPERIMENTAL SECTION

Spectroscopic and Magnetic Measurement

The infrared spectra were recorded on a Nicolet Fourier Transform IR, MAGNA-IR 500 spectrometer in the range of 500-4000 cm^{-1} using the KBr disc technique. UV-visible spectra were recorded on a Hewlett Packard (HP) 8453 spectrophotometer, maxima are listed in the form λ max (nm) (ε ($M^{-1}\cdot cm^{-1}$)). Magnetic measurements of complexes **2** and **3** were carried out on polycrystalline samples with a SQUID magnetometer. Molar magnetic susceptibility was recorded every 5 K in the range of 5-300 K with 10,000 Gauss external field.

Preparation of $[Ni_3(\mu_3\text{-dpa})_4(C_4O_4Me)](BF_4)$ 1

$AgBF_4$ (0.035 g, 0.172 mmol) was added to a 25 mL CH_2Cl_2 solution containing $[Ni_3(\mu_3\text{-dpa})_4Cl_2]$ (0.08 g, 0.086 mmol) at room temperature. The resulting solution was stirred for 30 minutes, then filtered. Solid squaric acid ($H_2C_4O_4$) (0.01 g, 0.086 mmol) was dissolved into the methanol solution. Two solutions were mixed together and stirred for two days. Solid powder were extracted with CH_2Cl_2 and re-crystallized from CH_2Cl_2/*n*-hexane solution. Deep purple crystals were obtained (Yield 71%). IR (KBr) ν = 1805 (C=O), 1686 (C=C) for methyl-squarate ion, 1591, 1562, 1541 (C=C) cm^{-1}. MS (FAB) *m/z* (%) 983 $[Ni_3(\mu_3\text{-dpa})_4(C_4O_4Me)]^+$, 856(15) $[Ni_3(\mu_3\text{-dpa})_4]^+$. The electronic spectrum (CH_2Cl_2 solution, 1.82×10^{-5} M) shows maxima at λ = 246 nm (ε = 4.26×10^4 M^{-1} cm^{-1}), 310 nm (ε = 3.39×10^4 M^{-1} cm^{-1}), 341 nm (ε = 3.65×10^4 M^{-1} cm^{-1}), 480 nm (ε = 2.31×10^3 M^{-1} cm^{-1}). Anal. Calcd for **1**•$4CH_2Cl_2$: C, 41.72; H, 3.07; N, 11.92. Found: C, 41.56; H, 2.93; N, 12.03.

Preparation of $[Ni_3(\mu_3\text{-dpa})_4(N_3)](PF_6)$ 2

$AgPF_6$ (0.042 g, 0.216 mmol) was added to a 20 mL CH_2Cl_2 solution containing $[Ni_3(\mu_3\text{-dpa})_4Cl_2]$ (0.1g, 0.108 mmol) at room temperature. The resulting solution was stirred for 30 minutes, then filtered. NaN_3 (0.007 g, 0.108 mmol) was added to the solution, and stirred for two days. Solid powder were extracted with CH_2Cl_2 and re-crystallized from CH_2Cl_2/*n*-hexane solution. Deep purple crystals were obtained (Yield 40%). IR (KBr) ν = 2097, 2045 (azide), 1603, 1592, 1549, (C=C) cm^{-1}. MS (FAB) *m/z* (%) 897(35) $[Ni_3(\mu_3\text{-dpa})_4(N_3)]^+$, 856(5) $[Ni_3(\mu_3\text{-dpa})_4]^+$. The electronic spectrum (CH_2Cl_2 solution, 1.82×10^{-5} M) shows maxima at λ = 241 nm (ε = 3.20×10^4 M^{-1} cm^{-1}), 315 nm (ε = 4.09×10^4 M^{-1} cm^{-1}), 351 nm (ε = 3.60×10^4 M^{-1} cm^{-1}), 406 nm (ε = 4.64×10^3 M^{-1} cm^{-1}), 517 nm (ε = 2.57×10^4 M^3 cm^{-1}). Anal. Calcd for **2**•$3CH_2Cl_2$: C, 50.00; H, 3.47; N, 18.22. Found: C, 50.19; H, 3.33; N, 18.53.

Preparation of $[Ni_3(\mu_3\text{-dpa})_4(N_3)_2]$ 3

NaN_3 (26 mg, 0.4 mmole) was added to the red-purple solution of $[Ni_3(\mu_3\text{-dpa})_4Cl_2]$ (92.8 mg, 0.1 mmole) in an Erlemeyer flask containing 30 mL of ethanol. Heating about 2-3 hrs and cooling to room temperature, deep-purple crystals were obtained at the bottom of the flask. The crystals were collected and extracted by CH_2Cl_2. The organic layer was concentrated, and a red-purple powder was obtained. The powder was re-crystallized from CH_2Cl_2/diethylether solution, and deep-purple crystals were obtained (Yield 80%). IR (KBr) ν = 2044 cm^{-1} (azide), 1596, 1586, 1543 (C=C). MS (FAB) [*m/z* (%)]: 897(2) $[Ni_3(\mu_3\text{-dpa})_4(N_3)]^+$, 856(5) $[Ni_3(\mu_3\text{-dpa})_4]^+$. Anal. Calcd for **3**•$1CH_2Cl_2\cdot1/2[O(C_2H_5)_2]$: C, 48.59; H, 3.70; N, 23.72. Found: C, 49.01; H, 3.48; N, 23.27.

Crystallographic Procedure

Crystal data for 1•$O(C_2H_5)_2$

A dark purple crystal of approximately 0.15 × 0.25 × 0.4 mm was mounted on a glass capillary. Data collection was carried out on a Siemens SMART diffractometer with a CCD detector with Mo radiation at room temperature. A preliminary orientation matrix and unit cell parameters were determined from 3 runs of 15 frames each. Each frame corresponds to a 0.3° scan in 15s, followed by spot integration and least-squares refinement. Data were measured using ω scan of 0.3° per frame for 20s until a complete hemisphere had been collected. Cell parameters were retrieved using SMART[15] software and refined with SAINT on all observed reflections. Data reduction was performed with the SAINT[16] software and corrected for Lorentz and polarization effects. Absorption corrections were applied with the program SADABS.[17] The structures were solved by the direct methods with the SHELX-93[18] program and refined by full-matrix least-squares methods on F^2 with SHEXLTL-PC V 5.03.[18] All non-hydrogen atomic positions were located in difference Fourier maps and refined anisotropically. Hydrogen atoms were placed in their geometrically generated positions. The detailed data collection and refinement of complex 1 are summarized in Table 1 and selected bond distances and angles are listed in Table 2. Other crystallographic data are given as Supporting Information.

Table 1. Crystallographic Data for **1**, **2** and **3**

	Compound		
	1·$O(C_2H_5)_2$	**2**·$3CH_2Cl_2$	**3**
formula	$Ni_3BF_4O_5N_{12}C_{49}H_{45}$	$Ni_3Cl_6PF_6N_{15}C_{43}H_{38}$	$Ni_3N_{18}C_{40}H_{32}$
fw	1144.91	1298.67	940.94
crystal system	monoclinic	monoclinic	monoclinic
space group	*C* 2/c	P 2_1/n	P 2_1/c
color	Dark purple	Dark purple	Dark purple
crystal size	0.15 × 0.25 × 0.40	0.25 × 0.30 × 0.70	0.25 × 0.35 × 0.50
a (Å)	19.9078(3)	13.323(4)	13.774(2)
b (Å)	13.2986(2)	23.217(3)	16.519(2)
c (Å)	37.6622(5)	17.528(5)	17.205(3)
β (°)	94.091(1)	94.42(3)	94.16(1)
V (Å^3)	9945.5(2)	5405(2)	3904.3(1)
Z	8	4	4
ρ_{calcd} (g·cm^{-3})	1.529	1.596	1.601
μ (cm^{-1})	11.99	14.35	14.95
$R(F_o)$; $R_w(F_o)$*($I > 2\sigma(I)$)	0.074; 0.172	0.066; 0.066	0.033; 0.034
$R(F_o)$; $R_w(F_o)$* (all data)	0.113; 0.194	0.165; 0.079	0.065; 0.037
GOF	1.089	1.56	1.39

* $R_w(F_o^2)$ for **1**, $R_w(F_o)$ for **2** and **3**

Table 2. Selected Bond Lengths (Å) and Angles (°) for **1**

Ni(1)-Ni(2)	2.400(1)	Ni(1)-N(1)	2.075(5)
Ni(2)-Ni(3)	2.403(1)	Ni(1)-N(4)	2.048(5)
Ni(1)-O(1)	2.146(5)	Ni(1)-N(7)	2.050(5)
Ni(3)-O(2)	2.075(4)	Ni(1)-N(10)	2.047(5)
O(1)-C(41)	1.182(7)	Ni(2)-N(2)	1.894(4)
O(2)-C(43)	1.261(7)	Ni(2)-N(5)	1.895(4)
O(3)-C(42)	1.178(8)	Ni(2)-N(8)	1.894(4)
O(4)-C(44)	1.350(8)	Ni(2)-N(11)	1.892(5)
O(4)-C(45)	1.350(8)	Ni(3)-N(3)	2.085(5)
C(41)-C(42)	1.495(9)	Ni(3)-N(6)	2.077(5)
C(42)-C(43)	1.499(9)	Ni(3)-N(9)	2.085(5)
C(43)-C(44)	1.446(9)	Ni(3)-N(12)	2.094(5)
C(44)-C(41)	1.51(1)		
Ni(1)···Ni(3)	**4.800**	**Ni(1)···Ni(3)'**	**8.548**
Ni(1)-Ni(2)-Ni(3)	176.51(4)		
Ni(2)-Ni(1)-O(1)	176.2(1)	Ni(2)-Ni(3)-O(3)	176.1(1)
Ni(1)-O(1)-C(41)	152.9(2)	Ni(3)-O(2)-C(43)	151.0(4)
C(42)-C(43)-C(44)	87.1(5)	O(1)-C(41)-C(42)	132.1(7)
C(44)-C(41)-C(42)	87.6(5)	O(2)-C(43)-C(44)	134.9(6)
C(41)-C(42)-C(43)	90.4(5)	O(3)-C(42)-C(43)	136.3(6)
C(43)-C(44)-C(41)	94.9(5)	O(4)-C(44)-C(41)	132.1(7)

Crystal data for 2·3CH_2Cl_2 and 3

Suitable single crystals were mounted on the glass capillary with approximation size of 0.25 × 0.30 × 0.70 mm and 0.25 × 0.30 × 0.50 mm for (**2**) and (**3**), respectively. Both measurements were made on a Nonius CAD4 diffractometer with graphite-monochromated MoKα radiation (λ = 0.7107 Å). The data were collected at room temperature using the ω-2θ scan technique to a maximum 2θ of 50°. Cell parameters were determined using 25 reflections in the 2θ ranges of 11.25° - 26.64° for **2** and 19.46° - 24.16° for **3**, respectively.

Table 3. Selected Bond Lengths (Å) and Angles (°) for **2**

Ni(1)-Ni(2)	2.389(2)	Ni(2)-Ni(3)	2.385(2)
Ni(1)-N(13)	2.029(7)	Ni(3)-N(15)	2.028(8)
N(13)-N(14)	1.162(10)	N(14)-N(15)	1.205(11)
Ni(1)-N(1)	2.063(8)	Ni(1)-N(4)	2.053(8)
Ni(1)-N(7)	2.066(8)	Ni(1)-N(10)	2.070(7)
Ni(2)-N(2)	1.887(7)	Ni(2)-N(5)	1.873(8)
Ni(2)-N(8)	1.862(8)	Ni(2)-N(11)	1.872(7)
Ni(3)-N(3)	2.082(7)	Ni(3)-N(6)	2.067(7)
Ni(3)-N(9)	2.071(8)	Ni(3)-N(12)	2.082(8)
Ni(1)···Ni(3)	**4.774**	**Ni(1)···Ni(3)'**	**5.930**
Ni(1)-Ni(2)-Ni(3)	179.46(7)	N(13)-N(14)-N(15)	178(1)
Ni(2)-Ni(1)-N(13)	177.4(2)	Ni(2)-Ni(3)-N(15)	178.1(3)
Ni(1)-N(13)-N(14)	131.8(7)	Ni(3)-N(15)-N(14)	135.8(7)

Table 4. Selected Bond Lengths (Å) and Angles (°) for **3**

Ni(1)-Ni(2)	2.4325(7)	Ni(2)-Ni(3)	2.4356(7)
Ni(1)-N(13)	2.031(3)	Ni(3)-N(15)	2.043(3)
N(13)-N(14)	1.083(5)	N(14)-N(15)	1.179(6)
N(16)-N(17)	1.152(5)	N(17)-N(18)	1.182(5)
Ni(1)-N(1)	2.075(3)	Ni(1)-N(4)	2.098(3)
Ni(1)-N(7)	2.075(3)	Ni(1)-N(10)	2.097(3)
Ni(2)-N(2)	1.899(3)	Ni(2)-N(5)	1.887(3)
Ni(2)-N(8)	1.891(3)	Ni(2)-N(11)	1.891(3)
Ni(3)-N(3)	2.089(3)	Ni(3)-N(6)	2.086(3)
Ni(3)-N(9)	2.087(3)	Ni(3)-N(12)	2.078(3)
Ni(1)···Ni(3)	**4.868**		
Ni(1)-Ni(2)-Ni(3)	178.67(3)		
Ni(2)-Ni(1)-N(13)	175.4(1)	Ni(2)-Ni(3)-N(16)	176.4(1)
Ni(1)-N(13)-N(14)	137.5(3)	Ni(3)-N(16)-N(17)	126.5(3)
N(13)-N(14)-N(15)	175.5(5)	N(16)-N(17)-N(18)	178.3(5)

Three intensity-control reflections were monitored every 3600s during the data collection. The intensity data were corrected for Lorentz and polarization effects, and refinement was performed using the counting statistics weighting scheme. An empirical absorption correction based on three azimuthal scans was also applied. The structures were solved using the direct methods and difference Fourier techniques, and refined by full-matrix least-squares methods. The non-hydrogen atoms were refined anisotropically, and the hydrogen atoms were included in an idealized geometry but not refined. The detailed data collection and refinement of complexes **2** and **3** are summarized in Table 1 and selected bond distances and angles are listed in Table 3 and 4, respectively. Other crystallographic data are given as Supporting Information. All calculations were carried out with the NRCVAX program[19] on the VAX Alpha station.

RESULTS AND DISCUSSION

Synthesis of Complexes 1-3

The starting material, $[Ni_3(\mu_3\text{-dpa})_4Cl_2]$, was synthesized according to the method reported in the literature.[2] Complexes **1** and **2** were synthesized *via* the axial-ligand-displacement method by adding two equivalents of $AgBF_4$ and $AgPF_6$, respectively, to pull away the Cl^- ligands of $[Ni_3(\mu_3\text{-dpa})_4Cl_2]$, after which the $C_4O_4^=$ (squarate) for **1** and N_3^- (azide) for **2** were added to coordinate at the axial positions of the $[Ni_3(\mu_3\text{-dpa})_4]^{2+}$ ions. The presence of the $C_4O_4Me^-$ ligand in **1** can be explained by the OMe^- ligand attacking the carbon atom of cyclic $C_4O_4^=$ in a methanol solution. Complex **3** was synthesized by the reaction of $[Ni_3(\mu_3\text{-dpa})_4Cl_2]$ and NaN_3 with a 1:4 molar ratio. Except for the axial ligands' vibrational mode, the infrared spectra of **1-3** are all similar to

those of the $[Ni_3(\mu_3\text{-dpa})_4Cl_2]$ complex[1] with the C-C vibrational modes at 1200-1600 cm^{-1} assignable to the pyridine ring. For complex **1**, two strong bands at 1686 and 1805 cm^{-1} are found which are the characteristic stretching vibration of the C=C and C=O bonds in the $C_4O_4Me^-$ ligand respectively. This result indicates a 1,2-dione form for the methoxysquarate ion which is consistent with the infrared spectra of $H_2C_4O_4$,[11] $[H(HC_4O_4)_2](NH_2Me_2)$,[12] and $[M(HC_4O_4)_2(H_2O)_2]$, (M = Mn, Fe).[13] In the case of complex **2**, two bands are observed at 2097 and 2045 cm^{-1} [$\nu_{as}(N_3)$]. Thus we may assume that the cation $[Ni_3(\mu_3\text{-dpa})_4]^{2+}$ is bridged with a μ-(1,3) azide ligand.[14] For complex **3**, the 2044 cm^{-1} band can be assigned to the terminal N_3 anion.

Structural Results

The details of data collection and refinement for complexes **1-3** are summarized in Table 1. As is in the case of $[Ni_3(\mu_3\text{-dpa})_4Cl_2]$,[1] the main $[Ni_3(\mu_3\text{-dpa})_4]^{2+}$ unit in these complexes is helical with the linear trinickel(II) chain being wrapped by four all-*syn* type dpa^- ligands. The selected bond distances and angles are listed in Tables 2-4 for complexes **1-3**, respectively. Except for the bond distances between the Ni atoms and the identity of the axial ligands, the central $[Ni_3(\mu_3\text{-dpa})_4]^{2+}$ units of the 3 complexes have much in common. The center Ni(II) ion is square planar with four short $Ni\text{-}N_{amido}$ distances in the range of 1.86-1.90 Å (Table 2-4), which is consistent with a low-spin (S = 0) square planar Ni(II) configuration system.[1,6-7,9-10] Two terminal Ni(II) ions are located in a square pyramidal environment with long $Ni\text{-}N_{pyridine}$ distances in the range of 2.05-2.10 Å. This is consistent with a high-spin (S = 1) Ni(II) configuration for the terminal Ni(II) ions.[1,6-7,9-10] In complex **1**, the one-dimensional polymeric chain is composed of alternating $[Ni_3(\mu_3\text{-dpa})_4]^{2+}$ units and methoxysquarate ligand ($C_4O_4Me^-$), where the methoxysquarate ion $(C_4O_4Me)^-$ acts as a μ-(1,3) bridged ligand that links two $[Ni_3(\mu_3\text{-dpa})_4]^{2+}$ units at the axial sites and each $[Ni_3(\mu_3\text{-dpa})_4]^{2+}$ unit provides two vacant axial sites to bond with two $(C_4O_4Me)^-$ ligands. The molecular drawing and a clearer view of the polymeric chain for complex **1** are shown in Figs. 1(a) and 1(b), respectively. Interestingly, all the methyl groups on the methoxysquarate of the polymeric chain are orientated in the same direction. According to the C-C and C-O distances listed in Table 2, a pattern of partial delocalization that extends from the coordinated oxygen O(1) *via* the methoxy-substituted carbon C(44) to the carbonyl oxygen O(2) is found (Fig. 1(a)). In the cyclo four-membered C_4 ring, the lengths of the C-C bonds that connect the methoxy group [C(41)-C(44) 1.437(9) Å, C(43)-C(44) 1.446(9) Å] are significantly shorter than the other two C-C bond distances [C(41)-C(42) 1.495(9) Å, C(42)-C(43) 1.499(9) Å]. This structure is close to a dione type which is similar to those found in the methoxysquarate complexes, $[M(C_4O_4Me)_2(H_2O)_4]$ (M = Mn, Co, Ni, Zn).[14]

In complexes **2** and **3**, the two axial sites of every $[Ni_3(\mu_3\text{-dpa})_4]^{2+}$ ion are both bonded with azide (N_3^-) ligands, where the azide (N_3^-) acts as a μ-(1,3) bridged ligand in **2** but as a terminal one in **3**. Similar to complex **1**, complex **2** is also a one-dimensional polymeric chain, consisting of $[Ni_3(\mu_3\text{-dpa})_4]^{2+}$ units and the azide ligands. The molecular structure of complex **2** is shown in Fig. 2. The azido bridge is not quite linear, the Ni-N-N angles being 131.8(7)° and 135.8(7)° for Ni(1) and Ni(3), respectively (Table 3). The azide ligand itself is asymmetric with N(13)-N(14) being 1.162(10) Å and N(14)-N(15) being 1.205(11) Å. Complex **3** is a linear trinickel(II) complex with two terminal azide ligands. Its structure is shown in Fig. 3. According to the selected bond distances and angles listed in Table 4, two terminal azide ligands are asymmetric with N-N distances of 1.083(5), 1.179(5) Å for N(13)-N(14), N(14)-N(15) and 1.152(5), 1.182(5) Å for N(16)-N(17), N(17)-N(18), respectively. The Ni-N-N angles are 137.5(5)° and 126.5(3)° for Ni(1) and Ni(3), respectively. It is previously reported that the terminal Ni-Ni distances in the pentanickel(II) $[Ni_5(\mu_5\text{-tpda})_4X_2]$ complexes are influenced by the σ-donor ability of the axial ligands.[7b] This influence by the axial ligands is even more obvious in the $[Ni_3(\mu_3\text{-dpa})_4X_2]$ complexes. A comparison of Ni-Ni distances for some trinickel(II) complexes with various axial ligands is listed in Table 5. Similar to the results found in the pentanickel complexes, the Ni-Ni distance is also the longest (2.4470(7) Å) when the axial ligand is a strong σ-donor ligand, CN^-, and is the shortest (2.39(1) Å) when the axial ligand is a solvent-coordinated ligand, CH_3CN. In addition, when comparing the Ni-Ni distances of two azide (N_3^-)-bonded complexes **2** and **3**, the Ni-Ni distances of 2.389(2) and 2.385(2) Å of the μ-1,3 bridged-azide **2** are significantly shorter than those (2.4325(7) and 2.4356(7) Å) of the terminal azide **3**. This result indicates that weakening in σ-donor ability from a terminal-azide ligand to a μ-1,3 bridged-azide ligand causes the shortening of the Ni-Ni distance.

Magnetic Studies

The molar magnetic susceptibilities χ_M (○) and magnetic moments μ_{eff} (□) with respect to temperature (T) for complexes **2** and **3** are plotted in Fig. 4 and 5, respectively. The χ_M values (4.060×10^{-3} for **2** and 3.148×10^{-3} for **3** at 300 K) decrease when temperature decreases, reaching a broad

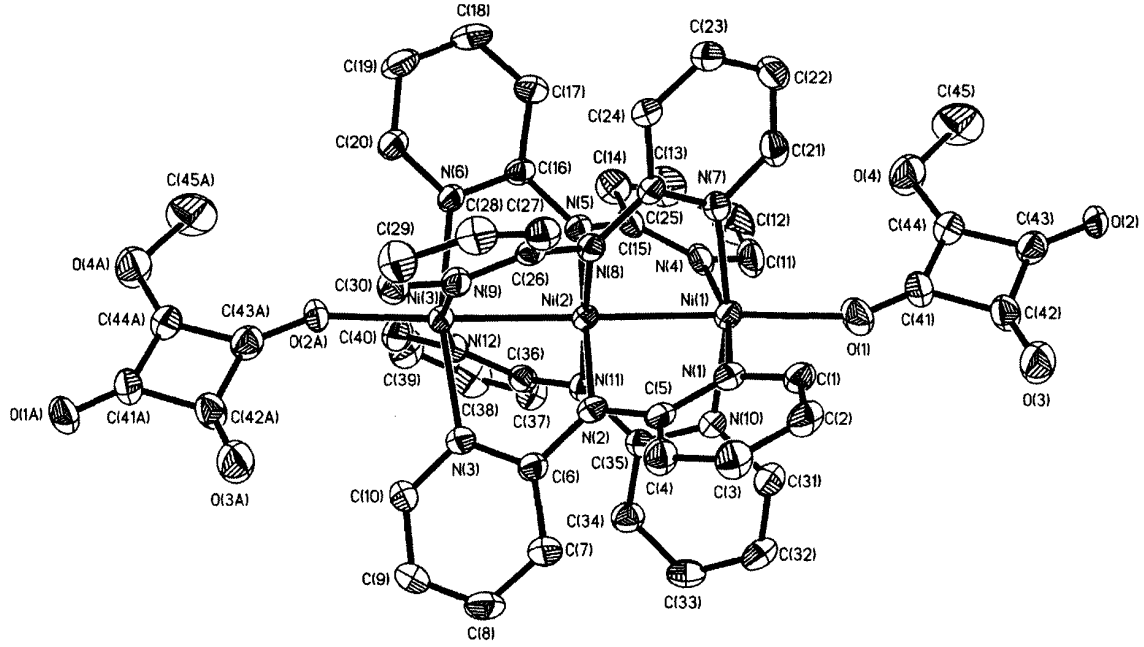

(a)

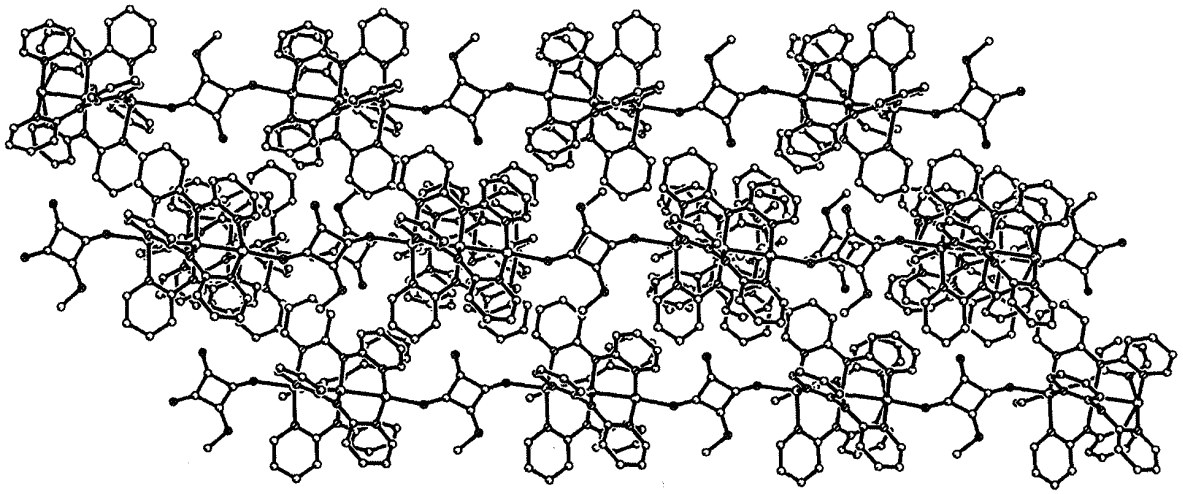

(b)

Fig. 1. (a) The crystal structure of $[Ni_3(\mu_3\text{-dpa})_4(\mu_{1,3}\text{-}C_4O_4(Me))](BF_4)$ **1**. (b) One-dimensional polymeric chain of complex **1**.

minimum ca 40 K for **2** and 35 K for **3**, with a χ_M minimum value of 1.984×10^{-3} for **2** and 1.284×10^{-3} for **3**, respectively. Below this temperatures, the χ_M increases continuously and reaches the values of 6.233×10^{-3} for **2** and 3.420×10^{-3} for **3** at 5 K. The theoretical simulation curves (solid line) agree well with the measurements. That means the electronic configurations derived from structural analyses are in a good agreement with the experimental magnetic measurements, with the central Ni(II) ion being in a low-spin (S = 0) state and two terminal NI(II) ions being in high spin (S = 1) states. The simulated curves of the molar magnetic susceptibility χ_M were fitted by the following equation:

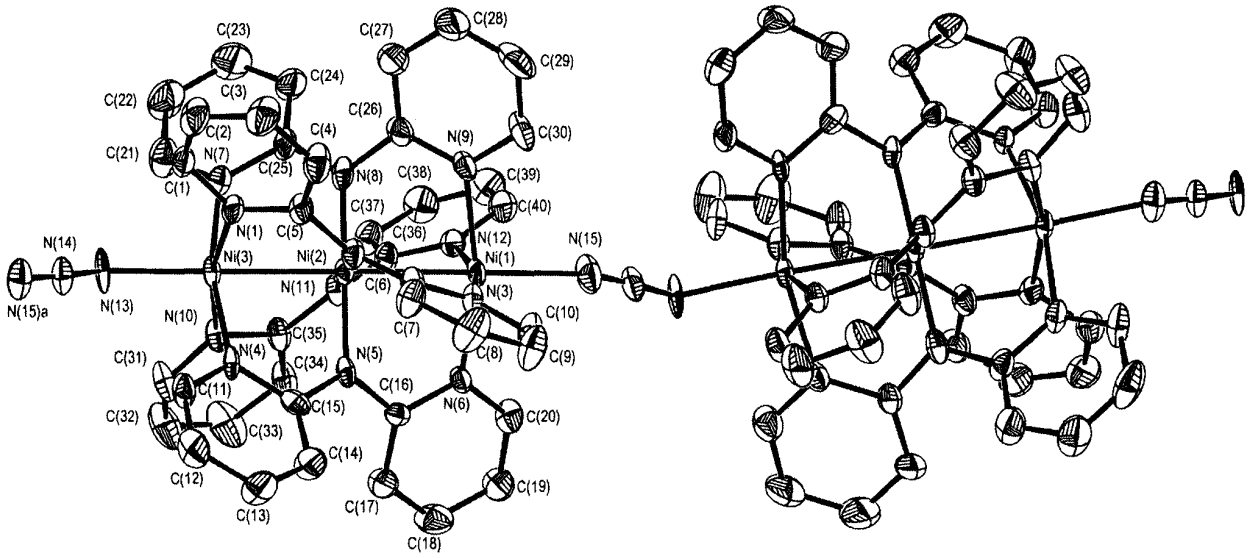

Fig. 2. The crystal structure of $[Ni_3(\mu_3\text{-dpa})_4(\mu_{1,3}\text{-}N_3)](PF_6)$ **2**.

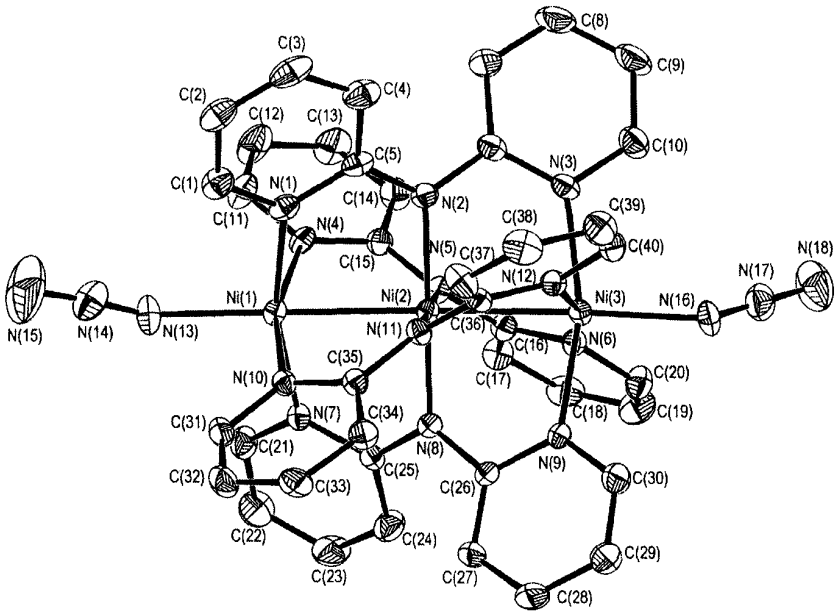

Fig. 3. The crystal structure of $[Ni_3(\mu_3\text{-dpa})_4(\mu_1\text{-}N_3)_2]$ **3**.

$\chi_M = (1-P)C'(2e^{2x} + 10e^{5x})/(1 + 3e^{2x} + 5e^{6x}) + P(2Ng^2\beta^2/3kT) + N_\alpha$

$C' = Ng^2\beta^2/k(T-\Theta)$ $x = J_{13}/kT$

$N = 6.022 \times 10^{23}$ g: g-factor

β = Bohr magneton k (Boltzmann): 0.695 cm^{-1} K^{-1}

T: abs temp (K) J_{13}: coupling const between Ni(1) and Ni(3)

Θ: Weiss temperature

P: relative content for paramagnetic impurity where spin state S = 1 is assume.

N_α: temperature-independent paramagnetism, TIP

The J_{13} values were obtained by minimizing the function $R = \Sigma(\chi_M^{calcd} - \chi_M^{obs})^2/\Sigma(\chi_M^{obs})^2$. The best fitting parame-

Table 5. Comparison of Ni-Ni Distances of $[Ni_3(\mu_3\text{-dpa})_4X_2]$ for Various Axial Ligands

Compound	Ni-Ni distance	reference
$[Ni_3(\mu_3\text{-dpa})_4(CN)_2]$	2.4470(7)	20
$[Ni_3(\mu_3\text{-dpa})_4Cl_2]$	2.443(1)	20
$[Ni_3(\mu_3\text{-dpa})_4(SC_4N_2H_3)_2]$	2.440(2)	20
$[Ni_3(\mu_3\text{-dpa})_4(N_3)_2]$	2.4325(7), 2.4356(7)	*
$[Ni_3(\mu_3\text{-dpa})_4(NCS)_2]$	2.4258(9)	20
$[Ni_3(\mu_3\text{-dpa})_4(NCCH_3)_2](PF_6)_2$	2.39(1)	20
$[Ni_3(\mu_3\text{-dpa})_4(C_4O_4Me)]_n(BF_4)_n$	2.400(1), 2.403(1)	*
$[Ni_3(\mu_3\text{-dpa})_4(N_3)]_n(PF_6)_n$	2.389(2), 2.385(2)	*

* This work

ters obtained are J_{13} = -95 cm^{-1}, g = 2.0, R = 7.17 × 10^{-4} for **2** and J_{13} = -97 cm^{-1}, g = 2.0, R = 5.64 × 10^{-4} for **3**. The negative

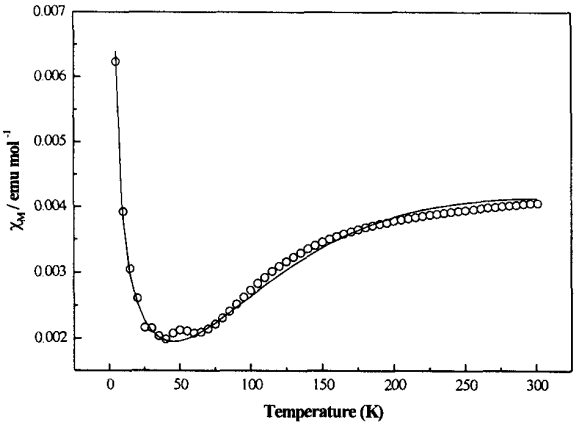

(a)

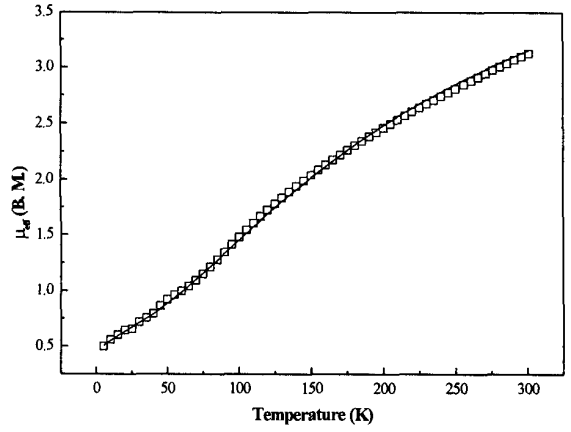

(b)

Fig. 4. Magnetic data for **2**. The solid line represents the results of theoretical simulation. (a) O indicates the observed χ_M; (b) □, the observed μ_{eff}.

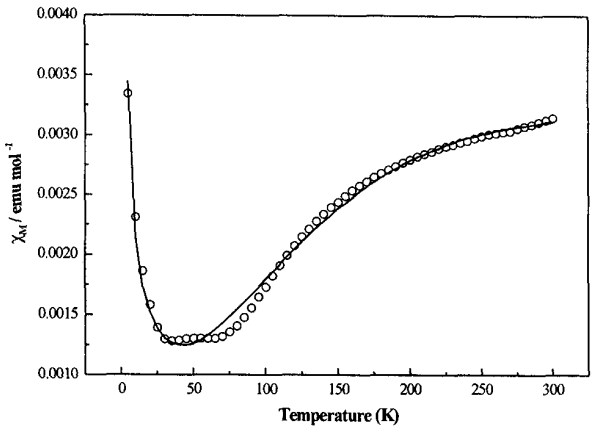

(a)

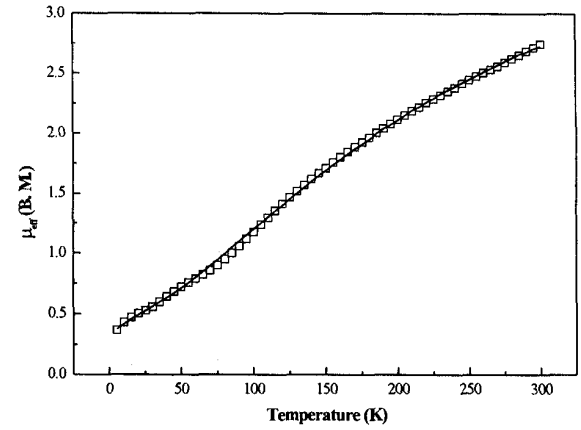

(b)

Fig. 5. Magnetic data for **3**. The solid line represents the results of theoretical simulation. (a) O indicates the observed χ_M; (b) □, the observed μ_{eff}.

J_{13} value of **3** reveal an antiferromagnetic interaction between two terminal high-spin nickel(II) ions by the intra- Ni(1)···Ni(3) through the Ni(2) ions with the Ni(1)···Ni(3) distance of 4.868 Å.[1,6-7,9-10] However, the antiferromagnetic interaction of complex **2** may be due to the super-exchange interaction by the intra- Ni(1)···Ni(3) through the Ni(2) ion (Ni(1)···Ni(3) 4.774 Å) or the inter- Ni(1)···Ni(3)' through the N_3^- ligand (Ni(1)···Ni(3)' 5.930 Å) or both through Ni(2) ion and N_3^- ligand.

CONCLUSION

Two one-dimensional polymeric trinickel(II) com-

plexes, $[Ni_3(\mu_3\text{-dpa})_4(C_4O_4(Me))(BF_4)$ **1** and $[Ni_3(\mu_3\text{-dpa})_4(N_3)](PF_6)$ **2**, are found with the $C_4O_4Me^-$ and N_3^- ligands both acting as a bridging unit to connect the $[Ni_3(dpa)_4]^{2+}$ block. The Ni-Ni distances of these two complexes are obviously shorter than those of the monomeric trinickel(II) complexes, $[Ni_3(\mu_3\text{-dpa})_4(X_2)]$. Magnetic susceptibility measurements of both complexes reveal an antiferromagnetic phenomenon. The values of the J coupling constants are -95 cm^{-1} and -97 cm^{-1} for **2** and **3**, respectively. These two complexes represent a new type of one-dimensional polymeric trinickel (II) complex.

ACKNOWLEDGEMENT

The authors thank the National Science Council of the Republic of China for financial support.

Received September 5, 2001.

Key Words

Metal-metal interaction; Polymeric trinickel complex; Anti-ferromagnetic interaction.

REFERENCES

1. (a) Wu, L. P.; Field, P.; Morrisey, T.; Murphy, C.; Nagle, P.; Hathaway, B.; Simmons, C.; Thornton, P. *J. Chem. Soc., Dalton Trans.* **1990**, 3835. (b) Pyrka, G. J.; El-Mekki, M.; Pinkerton, A. A. *J. Chem. Soc. Chem. Commun.* **1991**, 84. (c) Clérac, R.; Cotton, F. A.; Dunbar, K. R.; Murillo, C. A.; Pascual, I.; Wang, X. *Inorg. Chem.* **1999**, *38*, 2655.
2. Sheu, J. T.; Liu, C. C.; Chao, I.; Wang, C. C.; Peng, S. M. *Chem. Commun.* **1996**, 315.
3. (a) Cotton, F. A.; Daniels, L. M.; Murillo, C. A.; Pascual, I. *J. Am. Chem. Soc.* **1997**, *119*, 10223. (b) Cotton, F. A.; Daniels, L. M.; Murillo, C. A.; Wang, X. *Chem. Commun.* **1998**, 39. (c) Cotton, F. A.; Daniels, L. M.; Murillo, C. A.; Pascual, I. *Inorg. Chem. Commun.* **1998**, *1*, 1. (d) Clérac, R.; Cotton, F. A.; Daniels, L. M.; Dunbar, K. R.; Murillo, C. A.; Pascual, I. *Inorg. Chem.* **2000**, *39*, 748. (e) Clérac, R.; Cotton, F. A.; Daniels, L. M.; Dunbar, K. R.; Murillo, C. A.; Pascual, I. *Inorg. Chem.* **2000**, *39*, 752. (f) Clérac, R.; Cotton, F. A.; Daniels, L. M.; Dunbar, K. R.; Murillo, C. A.; Zhou, H. C. *Inorg. Chem.* **2000**, *39*, 3414.
4. (a) Yang, E. C.; Cheng, M. C.; Tsai, M. S.; Peng, S. M. *J. Chem. Soc., Chem. Commun.* **1994**, 2377. (b) Cotton, F. A.; Daniels, L. M.; Jordan, G. T. IV *Chem. Commun.* **1997**, 421. (c) Cotton, F. A.; Daniels, L. M.; Jordan, G. T. IV; Murillo, C. A. *J. Am. Chem. Soc.* **1997**, *119*, 10377. (d) Clerac, R.; Cotton, F. A.; Daniels, L. M.; Dumbar, K. R.; Murillo, C. A.; Pascual, I. *Inorg. Chem.* **2000**, *39*, 748. (e) Clerac, R.; Cotton, F. A.; Daniels, L. M.; Dumbar, K. R.; Murillo, C. A.; Pascual, I. *Inorg. Chem.* **2000**, *39*, 752. (f) Clérac, R.; Cotton, F. A.; Dunbar, K. R.; Lu, T.; Murillo, C. A.; Wang, X. *J. Am. Chem. Soc.* **2000**, *122*, 2272. (g) Clérac, R.; Cotton, F. A.; Dunbar, K. R.; Lu, T.; Murillo, C. A.; Wang, X. *Inorg. Chem.* **2000**, *39*, 3065. (h) Clérac, R.; Cotton, F. A.; Daniels, L. M.; Dunbar, K. R.; Kirschbaum, K.; Murillo, C. A.; Pinkerton, A. A.; Schultz, A. J.; Wang, X. *J. Am. Chem. Soc.* **2000**, *122*, 2272.
5. Aduldecha, S.; Hathaway, B. *J. Chem. Soc., Dalton Trans.* **1991**, 993.
6. Lai, S. Y.; Lin, T. W.; Chen, Y. H.; Wang, C. C.; Lee, G. H.; Yang, M. H.; Leung, M. K.; Peng, S. M. *J. Am. Chem. Soc.* **1999**, *121*, 250.
7. (a) Shieh, S. J.; Chou, C. C.; Lee, G. H.; Wang, C. C.; Peng, S. M. *Angew. Chem. Int. Ed. Engl.*, **1997**, *36*, 56. (b) Wang, C. C.; Lo, W. C.; Chou, C. C.; Lee, G. H.; Chen, J. M.; Peng, S. M. *Inorg. Chem.* **1998**, *37*, 4059.
8. Chang, H. C.; Li, J. T.; Lin, J. T.; Wang, C. C.; Lee, H. C.; Lee, G. H.; Peng, S. M. *Eur. J. Inorg. Chem.* **1999**, 1243.
9. Chen, H. C.; Lee, C. C.; Wang, C. C.; Lee, G. H.; Lai, S. Y.; Li, F. Y.; Mou, C. Y.; Peng, S. M. *Chem. Commun.* **1999**, 1667.
10. Peng, S. M.; Wang, C. C.; Jang, Y. L.; Chen, Y. H.; Li, F. Y.; Mou, C. Y.; Leung, M. K. *Journal of Magnetism and Magnetic Materials*, **2000**, *209*, 80.
11. Wang, Y.; Stucky, G. D.; Williams, J. M. *J. Chem. Soc. Perkin Trans. II* **1974**, 35.
12. Wang, Y.; Stucky, G. D. *J. Chem. Soc. Perkin Trans. II* **1974**, 925.
13. Lee, C. R.; Wang, C. C.; Wang, Y. *Acta. Cryst.* **1996**, *B52*, 966.
14. Hosein, H. A.; Jaggernauth, H.; Alleye, B. D.; Hall, L. A.; White, A. J. P.; Williams, D. J. *Inorg. Chem.* **1999**, *38*, 3716.
15. *SMART V 4.043 Software for the CCD Detector System*; Siemens Analytical Instruments Division: Madison, WI, 1995.
16. *SAINT V 4.035 Software for the CCD Detector System*; Siemens Analytical Instruments Division: Madison, WI, 1995.

17. Sheldrick, G. M. *SHELXL-93, Program for the Refinement of Crystal Structures*; University of Göttingen: Göttingen, Germany, 1993.
18. *SHELXTL 5.03 (PC-Version), Program Liberary for Structure Solution and Molecular Graphics*; Siemens Analytical Instruments Division: Madison, WI, 1995.
19. Gabe, E. J.; Le Page, Y.; Charland, J. P.; Lee, F. L.; White, P. S. *J. Appl. Cryst.* **1989**, *22*, 384.
20. Lo, W. C. Ph.D. Thesis, National Taiwan University, 1996.